1-7-2008

Giant intrinsic carrier mobilities in graphene and its bilayer

S. V. Morozov
University of Manchester

K. S. Novoselov
University of Manchester

M. I. Katsnelson
University of Nijmegen

F. Schedin
University of Manchester

D. C. Elias
University of Manchester

See next page for additional authors

Authors
S. V. Morozov, K. S. Novoselov, M. I. Katsnelson, F. Schedin, D. C. Elias, John A. Jaszczak, and A. K. Geim

Giant Intrinsic Carrier Mobilities in Graphene and Its Bilayer

S. V. Morozov,[1,2] K. S. Novoselov,[1] M. I. Katsnelson,[3] F. Schedin,[1] D. C. Elias,[1] J. A. Jaszczak,[4] and A. K. Geim[1,*]

[1]*Manchester Centre for Mesoscience and Nanotechnology, University of Manchester, Manchester M13 9PL, United Kingdom*
[2]*Institute for Microelectronics Technology, 142432 Chernogolovka, Russia*
[3]*Institute for Molecules and Materials, University of Nijmegen, 6525 ED Nijmegen, The Netherlands*
[4]*Department of Physics, Michigan Technological University, Houghton, Michigan 49931, USA*

(Received 3 November 2007; published 7 January 2008)

We have studied temperature dependences of electron transport in graphene and its bilayer and found extremely low electron-phonon scattering rates that set the fundamental limit on possible charge carrier mobilities at room temperature. Our measurements show that mobilities higher than 200 000 $cm^2/V\,s$ are achievable, if extrinsic disorder is eliminated. A sharp (thresholdlike) increase in resistivity observed above ~200 K is unexpected but can qualitatively be understood within a model of a rippled graphene sheet in which scattering occurs on intraripple flexural phonons.

DOI: 10.1103/PhysRevLett.100.016602 PACS numbers: 72.10.−d, 72.15.Lh

Graphene exhibits remarkably high electronic quality such that charge carriers in this one-atom-thick material can travel ballistically over submicron distances [1]. Electronic quality of materials is usually characterized by mobility μ of their charge carriers, and values of μ as high as 20 000 $cm^2/V\,s$ were reported for single-layer graphene (SLG) at low temperatures (T) [2–5]. It is also believed that μ in the existing samples is limited by scattering on charged impurities [6] or microscopic ripples [3,7]. Both sources of disorder can in principle be eliminated or reduced significantly. There are, however, intrinsic scatterers such as phonons that cannot be eliminated at room T and, therefore, set a fundamental limit on electronic quality and possible performance of graphene-based devices. How high is the intrinsic mobility μ_{in} for graphene at 300 K? This is one of the most important figures of merit for any electronic material, but it has remained unknown.

In this Letter, we show that electron-phonon scattering in graphene and its bilayer is so weak that, if the extrinsic disorder is eliminated, room-T mobilities ~200 000 $cm^2/V\,s$ are expected over a technologically relevant range of carrier concentration n. This value exceeds μ_{in} known for any other semiconductor [8]. In particular, our measurements show that away from the neutrality point (NP) resistivity ρ of SLG has two components: in addition to the well-documented contribution $\rho_L = 1/ne\mu$ due to long-range disorder [6,7], we have identified a small but notable n-independent resistivity ρ_S indicating the presence of short-range scatterers [6,7,9]. We have also found that ρ_L does not depend on T below 300 K, whereas ρ_S exhibits a sharp rise above ~200 K [10]. The latter contradicts to the existing theories [11] that expect a linear T dependence. We attribute this behavior to flexural (out-of-plane) phonons [12] that are excited inside ripples. Bilayer graphene (BLG) samples exhibited no discernible T dependence of μ away from NP, yielding even higher μ_{in}. These findings provide an important benchmark for the research area and indicate that μ in graphene systems can be orders of magnitude higher than the values achieved so far. The reported measurements are also important for narrowing dominant scattering mechanisms in graphene, which remain hotly debated [3–7,11,13].

The studied devices were prepared from graphene obtained by micromechanical cleavage of graphite on top of an oxidized Si wafer (usually, 300 nm of SiO_2) [14]. Single- and bilayer crystallites were initially identified by their optical contrast [15], verified in some cases by Raman and atomic-force microscopy [2,14,16] and always cross-checked by measurements in high magnetic fields B, where SLG and BLG exhibited two distinct types of the quantum Hall effect [2,17]. To improve homogeneity, our standard Hall bar devices [1–3] were annealed at 200 °C in a H_2-Ar mixture [18] and, then, inside a measurement cryostat at 400 K in He. To avoid accidental breakdown, gate voltages V_g were limited to ± 50 V ($n \propto \alpha V_g$ with $\alpha \approx 7.2 \times 10^{10}$ cm^{-2}/V [1–5]). The measurements discussed below were carried out by the standard lock-in technique and refer to 7 SLG and 5 BLG devices with μ between 3000 and 15 000 $cm^2/V\,s$.

Figure 1 shows a characteristic behavior of $\rho(V_g)$ in SLG. The device exhibits a sharp peak close to zero V_g (≈ -0.2 V), indicating little chemical doping [3]. Conductivity $\sigma = 1/\rho$ is a notably sublinear function of V_g in this device. Both linear and sublinear behaviors were reported previously [2–5]. To this end, if we subtract a constant resistivity ρ_S (≈100 Ω in Fig. 1), then $\sigma_L = 1/[\rho(V_g) - \rho_S]$ becomes perfectly linear over the whole range of positive and negative V_g, except for the immediate vicinity of NP (<± 3 V). This linearization procedure was found to work extremely well for all our devices [the only exception was occasional devices with strongly distorted $\rho(V_g)$ indicating macroscopic inhomogeneity [1]]. Furthermore, we digitized a number of curves in recent literature [4,5] and found the approach equally successful. This shows that resistivity of doped graphene can empirically be described by two contributions: $\rho_L \propto 1/n$ and ρ_S

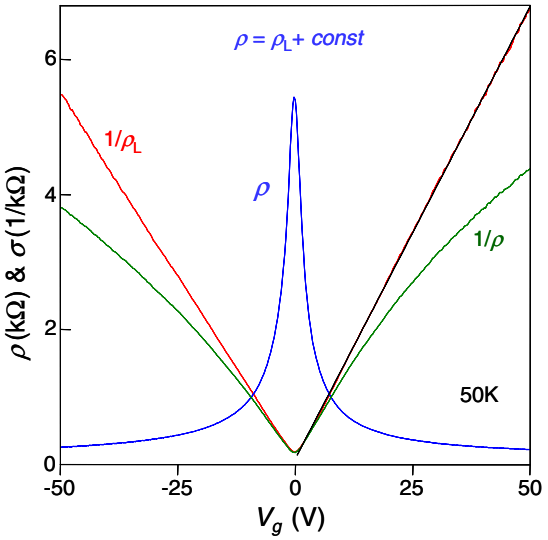

FIG. 1 (color online). Resistivity ρ (blue curve) and conductivity $\sigma = 1/\rho$ (green curve) of SLG as a function of gate voltage. If we subtract a constant of $\approx$100 Ω (used here as a fitting parameter), the remaining part $\rho_L(V_g)$ of resistivity becomes inversely proportional to V_g (red curve). The thin black line (on top of the red curve for $V_g > 0$) is to emphasize the linearity (the red curve is equally straight for negative V_g). The particular device was 1 μm wide, and $T = 50$ K was chosen to be high enough to suppress universal conductance fluctuations, still visible on the curves.

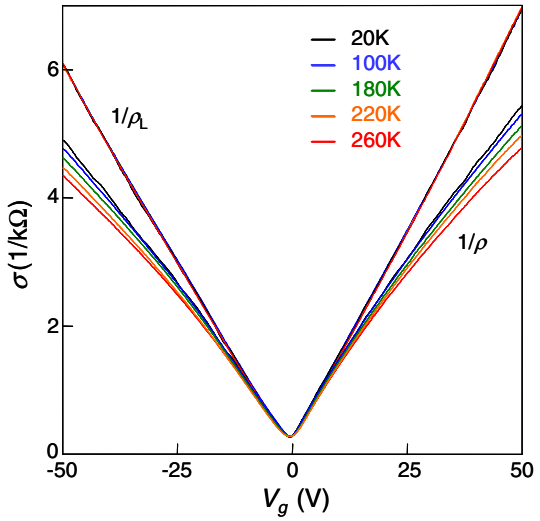

FIG. 2 (color online). Electron transport in graphene below 300 K can be described by the empirical expression $\rho(V_g, T) = \rho_L(V_g) + \rho_S(T)$ where ρ_S is independent of V_g but varies with T. After subtracting ρ_S that for this sample changed from $\approx$40 Ω at low T to $\approx$70 Ω at 260 K, the resulting curves $\sigma_L(V_g) = 1/\rho_L(V_g)$ became indistinguishable (the cluster marked $1/\rho_L$ consists of 5 such curves). The experiments were carried out in a field of 0.5 T to ensure that weak localization corrections (rather small [1,22] but still noticeable) do not contribute into the reported T dependences.

independent of n due to long- and short-range scatterers, respectively [3–7,9]. The latter contribution varies from sample to sample and becomes more apparent in high-μ samples. This observation resolves the controversy about the varying (linear vs sublinear) behavior reported in different experiments [2–5].

With this procedure in hand, it is now easier to describe T dependence of graphene's conductivity. Figure 2 shows that $\sigma(V_g)$ curves become increasingly sublinear with increasing T. However, after linearization, the resulting curves (with ρ_S subtracted) become essentially indistinguishable away from NP, collapsing onto a single curve $\sigma_L \propto |V_g|$ independently of T (<300 K; at higher T, we observed clear changes in the shape of $\sigma_L(V_g)$ curves, which indicates that the phonon contribution can no longer be described by ρ_S independent of n). The extracted values of ρ_S increase with T as shown in Fig. 3 for 4 different devices. One can see that their T dependent parts, $\Delta\rho_S = \rho_S(T) - \rho_S(0)$, behave qualitatively similar, despite different $\rho_S(0)$ at liquid-helium T. There is a slow (probably, linear) increase in ρ_S at low T but, above 200 K, it rapidly shoots up (as T^5 or quicker). The latter T dependence is inconsistent with scattering on acoustic phonons [11]. Note that $\Delta\rho_S$ does not exceed $\approx$ 50 Ω at 300 K, yielding μ_{in} between $\sim$40 000 and 400 000 cm^2/V s for characteristic V_g between 5 and 50 V (n between $\sim$3 and 30 $\times$ 10^{11} cm^{-2}).

Now we turn to BLG. A typical behavior of its conductivity is shown in Fig. 4. BLG exhibits $\sigma(V_g)$ qualitatively similar to SLG's: away from NP, $\sigma_L \propto |V_g|$ yielding a constant μ of between 3000 and 8000 cm^2/V s for our devices. This behavior (not reported before) is rather surprising because BLG's spectrum neither is similar to the conical spectrum of SLG [1,17] nor can it be considered parabolic (the measured cyclotron mass varies strongly with n [19]). As for T dependence in BLG, its only pronounced feature is a rapid decrease in ρ around NP such that the peak value changes by a factor of 3 between liquid helium to room T. The inset of Fig. 3 shows this dependence in more detail and compares it with the weak, nonmonotonic behavior observed at NP in SLG. The origin of this pronounced difference between graphene and its bilayer lies in their different density of states near NP, which vanishes for SLG but is finite in BLG [1]. For SLG, the concentration of thermally excited carriers Δn_T can be estimated as $(T/\hbar v_F)^2$, whereas in BLG it is $\sim Tm/\hbar^2$ (v_F is the Fermi velocity in SLG and m the effective mass in BLG [17,19]). In the latter case, $\Delta n_T \approx 10^{12}$ cm^{-2} at room T, an order of magnitude larger than for SLG. The data in Fig. 3 (inset) are in agreement with this consideration. The weak T dependence at NP is a unique feature of SLG and can be employed to distinguish SLG from thicker [14,20] crystallites.

Away from NP, we have never observed any sign of decrease in BLG's conductivity with increasing T. Comparison of Figs. 2 and 4 clearly illustrates that

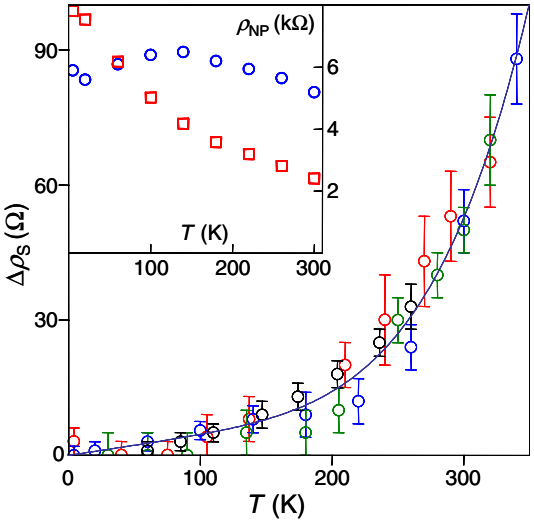

FIG. 3 (color online). T-dependent part of resistivity for 4 SLG samples (symbols). The accuracy of measuring $\Delta\rho_S$ was limited by mesoscopic fluctuations at low T and by gate hysteresis above 300 K. The hysteresis appeared when V_g was swept by more than 20 V. To find $\Delta\rho_S$ at higher T, we recorded ρ as a function of n (found from simultaneous Hall measurements). The solid curve is the best fit by using a combination of T and T^5 functions, which serves here as a guide to the eye. One of the samples (green circles) was made on the top 200 nm of SiO_2 covered by further 100 nm of polymethylmethacrylate (PMMA) and exhibited $\mu \approx 7000$ cm^2/V s. The same values of μ for SiO_2 and PMMA substrates probably rule out charged impurities in SiO_2 as the dominant scattering mechanism for graphene. The inset shows T dependence of maximum resistivity ρ_{NP} (at the neutrality point) for SLG and BLG (circles and squares, respectively). Note a decrease in ρ_{NP} with decreasing T below 150 K for SLG, which is a generic feature seen in many samples.

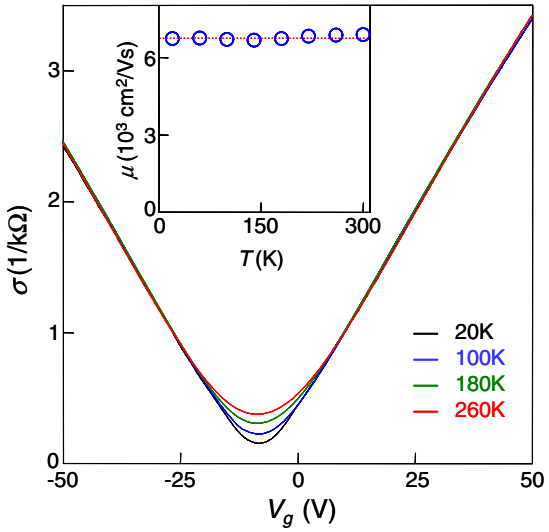

FIG. 4 (color online). T dependence in bilayer graphene. At the neutrality point, σ rapidly increases with T but, away from it, no changes are seen. $\sigma(V_g)$ exhibits a small sublinear contribution that can also be interpreted in terms of a constant ρ_S. The inset plots nominal values of μ found from linear fits of $\sigma_L(V_g)$ at $V_g > 20$ V away from NP and using $\rho_S \approx 50$ Ω. Here, μ does not change within $\approx 2\%$ and, if anything, shows a slight increase at higher T. The measurements were carried out at $B = 0.5$ T to suppress a small contribution of weak localization.

T-dependent scattering in BLG is substantially weaker than in SLG. Further measurements (Fig. 4) have shown that phonons do not contribute into BLG's μ within our experimental accuracy of $<2\%$. This yields $\mu_{in} > 300\,000$ cm^2/V s and a mean-free path of several microns at 300 K.

Let us now try to understand the observed T dependence of $\Delta\rho_S$ (Fig. 3). On one hand, it is partially consistent with scattering by in-plane phonons [11] in the sense that they lead to resistivity independent of n. On the other hand, such phonons give rise only to $\Delta\rho_S \propto T$, in clear disagreement with the measurements above 200 K. These are rather general predictions and can be understood as follows. Because $v_F/v \approx 10^3$ (v is the speed of sound), the Fermi wavelength λ_F in our experiments exceeds the spatial scale associated with thermal phonons, $\approx 1/q_T$, at $T > 10$ K ($q_T \approx T/v$ is the typical wave vector). This means that the scattering has a short-range character, leading to $\Delta\rho_S$ independent of n [7,11]. Furthermore, the standard momentum and energy conservation considerations yield that only phonons with wave vectors $\sim k_F$ provide efficient (large-angle) scattering. The number of such phonons is $\propto T$ (given by the Boltzmann distribution in the limit $T \gg qv$) and, accordingly, $\Delta\rho_S \propto T$ [11], which can explain only our low-T data. We also considered other T-dependent mechanisms such as flexural phonons [12,21], electron-electron scattering, and umklapp processes, and they cannot explain the experimental behavior.

In the absence of a theory able to describe the rapid increase in $\Delta\rho_S$, we point out that the behavior is consistent with scattering on flexural phonons confined *within* ripples. Ripples are a common feature of cleaved graphene [18,22], suggesting that the atomic sheet is not fully bound to a substrate (as illustrated in Ref. [23]) and, therefore, may exhibit local out-of-plane vibrations. First, because a characteristic size of ripples, $d \sim 10$ nm, is typically smaller than λ_F [18,22], such vibrations induce predominantly short-range scattering. Second, at low T ($q_T \ll 2\pi/d$), few flexural modes can be excited inside ripples but, as T increases and typical wavelengths become shorter, more and more flexural phonons come into play. It was suggested [7] that electron scattering in graphene is dominated by static ripples quenched from the flexural-phonon disorder when graphene was deposited on a substrate at room T (there are also short-range ripples induced by substrate's roughness [18]), which implies that any appreciable number of intraripple phonons start appearing only around room T. In fact, the observed behavior was predicted by Das Sarma and co-workers who—advocating for charged impurities as dominant scatterers in graphene [6,13]—noted that the model of quenched-ripple disorder [7] implied "strong temperature dependence (above a cer-

tain quenching temperature of about 100 K)—an effect that has not been observed in the experiments'' [13]. This is exactly the experimental behavior reported here.

To estimate scattering rates $1/\tau$ for intraripple flexural phonons, one has to take into account two-phonon scattering processes because out-of-plane deformations modulate electron hopping only in the second order [7,12]. For our case of $q \gg k_F$, we have found [21]

$$\frac{1}{\tau} \cong \frac{\pi t'^2 k_F a^2}{8 v_F} \sum_{q \geq q_c} \frac{q^4}{M^2 \omega_q^2} \left(e^{\beta \omega_q} + \frac{2\beta\omega_q}{1 - e^{-2\beta\omega_q}} \right) \times \frac{1}{(e^{\beta\omega_q} - 1)^2},$$

where $\beta = \hbar/T$, M is the mass of a carbon atom, a the lattice constant, $\omega_q \propto q^2$ the flexural-phonon frequency, and t' the derivative of the nearest-neighbor hopping integral with respect to deformation [7]. The integration goes over intraripple phonons that have q larger than the cutoff wave vector $q_c \approx 2\pi/d$ imposed by the quenching. At low T, no flexural vibrations are allowed inside ripples ($\delta\rho \approx 0$), whereas in the high-T limit ($q_T \gg 2\pi/d$) the above expression allows the estimate $\delta\rho \approx (\hbar/e^2)(Td/2\pi\kappa a)^2$, yielding $\delta\rho \sim 100$ to 1000 Ω at 300 K ($\kappa \approx 1$ eV is the bending rigidity of graphene [7]). The rapid increase in $\Delta\rho_S$ above 200 K can be attributed to transition between the low- and high-T limits. The absence of any appreciable T dependence in BLG is also consistent with the model, as BLG is more rigid and exhibits weaker rippling [22].

In summary, weak T dependence of electron transport in graphene and its bilayer yields $\mu_{\text{in}} > 200\,000$ cm^2/V s. The rapid rise in the small T-dependent part of ρ in SLG lends support for the model of quenched-ripple disorder as an important scattering mechanism. The model suggests that the observed T dependence is extrinsic and can probably be reduced together with ripples by depositing graphene on liquid-nitrogen-cooled substrates. If scattering on in-plane phonons does not increase in a flatter graphene sheet, μ_{in} could be truly colossal.

We are grateful to M. Dresselhaus who stimulated this work by repeatedly raising the question about graphene's intrinsic mobility. We also thank A. Castro Neto, S. Das Sarma, F. Guinea, and V. Falko for useful discussions. This work was supported by EPSRC (U.K.) and the Royal Society.

Note added.—After the manuscript was submitted, Fratini and Guinea [24] suggested that the observed strong T dependence could alternatively be explained by scattering on surface phonons in the SiO_2 substrate, and this explanation was later used by Chen *et al.* [25] to analyze their experiment. The found agreement between the theory and both experiments is striking, but let us note that two of the reported SLG samples were on top of 100 nm of PMMA (not SiO_2; see Fig. 3), and it would be fortuitous if the materials with so different polarizibility induce the same surface phonon scattering.

*geim@man.ac.uk

[1] For review, see A. K. Geim and K. S. Novoselov, Nat. Mater. **6**, 183 (2007); A. H. Castro Neto *et al.*, arXiv:0709.1163.
[2] K. S. Novoselov *et al.*, Nature (London) **438**, 197 (2005); Y. Zhang *et al.*, Nature (London) **438**, 201 (2005).
[3] F. Schedin *et al.*, Nat. Mater. **6**, 652 (2007).
[4] Y. W. Tan *et al.*, Phys. Rev. Lett. **99**, 246803 (2007).
[5] J. H. Chen *et al.*, arXiv:0708.2408.
[6] K. Nomura and A. H. MacDonald, Phys. Rev. Lett. **96**, 256602 (2006); T. Ando, J. Phys. Soc. Jpn. **75**, 074716 (2006); E. H. Hwang, S. Adam, and S. Das Sarma, Phys. Rev. Lett. **98**, 186806 (2007).
[7] M. I. Katsnelson and A. K. Geim, Phil. Trans. R. Soc. A **366**, 195 (2008).
[8] T. Durkop *et al.*, Nano Lett. **4**, 35 (2004).
[9] E. Fradkin, Phys. Rev. B **33**, 3263 (1986); Y. Zheng and T. Ando, Phys. Rev. B **65**, 245420 (2002).
[10] Weak T dependence in SLG was noted in Refs. [1,2], E. W. Hill *et al.*, IEEE Trans. Magn. **42**, 2694 (2006), and Y. W. Tan *et al.*, Eur. J. Phys. Special Topics **148**, 15 (2007), but neither quantified nor discussed.
[11] T. Stauber, N. M. R. Peres, and F. Guinea, Phys. Rev. B **76**, 205423 (2007); F. T. Vasko and V. Ryzhii, Phys. Rev. B **76**, 233404 (2007); S. Das Sarma (private communication).
[12] E. Mariani and F. von Oppen, arXiv:0707.4350. Small-angle scattering by acoustic phonons ($\propto T^4$) mentioned in the paper is valid in the low-T limit ($T < 10$ K).
[13] S. Adam, E. H. Hwang, and S. Das Sarma, arXiv:0708.0404.
[14] K. S. Novoselov *et al.*, Science **306**, 666 (2004); Proc. Natl. Acad. Sci. U.S.A. **102**, 10451 (2005).
[15] P. Blake *et al.*, Appl. Phys. Lett. **91**, 063124 (2007).
[16] A. C. Ferrari *et al.*, Phys. Rev. Lett. **97**, 187401 (2006).
[17] K. S. Novoselov *et al.*, Nature Phys. **2**, 177 (2006); E. McCann and V. I. Fal'ko, Phys. Rev. Lett. **96**, 086805 (2006).
[18] M. Ishigami *et al.*, Nano Lett. **7**, 1643 (2007).
[19] E. V. Castro *et al.*, Phys. Rev. Lett. **99**, 216802 (2007).
[20] S. V. Morozov *et al.*, Phys. Rev. B **72**, 201401 (2005).
[21] Flexural phonons lead to $\delta\rho \propto T^2/n$. The expression can be derived by the same technique that was used for two-magnon scattering in half-metallic ferromagnets [V. Yu. Irkhin and M. I. Katsnelson, Eur. Phys. J. B **30**, 481 (2002)]. In Ref. [7], scattering on ripples was considered by assuming that they were static, resulting from flexural phonons quenched during graphene's deposition on a room-T substrate. A careful quantum analysis leads to the same result for dynamic ripples (flexural phonons), if T is much larger than their energy at wave vectors $\sim k_F$. The latter is valid for $T > 1$ K. In the opposite low-T limit, scattering on flexural phonons was studied in Ref. [12].
[22] S. V. Morozov *et al.*, Phys. Rev. Lett. **97**, 016801 (2006); J. C. Meyer *et al.*, Nature (London) **446**, 60 (2007); E. Stolyarova *et al.*, Proc. Natl. Acad. Sci. U.S.A. **104**, 9209 (2007).
[23] E. A. Kim and A. H. Castro Neto, arXiv:cond-mat/0702562.
[24] S. Fratini and F. Guinea, arXiv:0711.1303v1.
[25] J. H. Chen *et al.*, arXiv:0711.3646.